Preparation, Solution Dynamics, and X-ray Structure of Bis(pentamethylcyclopentadienyl)actinide Complexes of Chelating Phosphorus Ylides

Roger E. Cramer,* Steven Roth, Frank Edelmann, Michael A. Bruck, Kim C. Cohn, and John W. Gilje*

Chemistry Department, University of Hawaii, Honolulu, Hawaii 96822

Received August 16, 1988

The reaction of $Cp^*_2AnCl_2$ ($Cp^* = C_5Me_5$; An = U or Th) with 1 equiv of $Li(CH_2)(CH_2)PRR'$ (**a**, R = Me, R′ = Ph; **b**, R = R′ = Ph; **c**, R = R′ = Me) produces $Cp^*_2An(Cl)[(CH_2)(CH_2)PRR']$ (**1**, An = U; **2**, An = Th), in good yield. The structures of $Cp^*_2U(Cl)[(CH_2)(CH_2)P(Ph)R]$ (**1a**, R = Me; **1b**, R = Ph) have been determined by X-ray crystallography. **1a** crystallizes in the monoclinic space group $P2_1/c$ with a = 13.963 (8) Å, b = 11.904 (2) Å, c = 17.541 (3) Å, β = 103.17 (3)°, Z = 4, V = 2839 (2) Å^3, R = 0.0402, and R_g = 0.0439 and in the triclinic space group $P\bar{1}$ with a = 11.725 (9) Å, b = 14.625 (7) Å, c = 8.547 (3) Å, α = 98.41 (4)°, β = 95.54 (5)°, γ = 94.78 (5)°, Z = 2, V = 1436 (1) Å^3, R = 0.0689, and R_g = 0.0882. **1b** crystallizes in the monoclinic space group $P2_1/n$ with a = 8.763 (8) Å, b = 19.579 (5) Å, c = 18.574 (5) Å, β = 93.60 (4)°, Z = 4, V = 3180 (3) Å^3, R = 0.074, and R_g = 0.0822. The U(IV) is nine-coordinate, bound by two Cp* groups and a chloro ligand and chelated by the phosphoylide through two CH_2 groups. The average $U-CH_2$ bond length is 2.60 (1) Å. ^1H NMR studies of the diamagnetic Th(IV) compounds show two types of CH_2 groups at low temperature that undergo rapid exchange at higher temperature. The fluxional behavior has been interpreted in terms of a series of metal–carbon bond breaking, rotation, and recombination processes. The $\Delta G^{\ddagger}$ for the exchange within **2a** is 15.4 ± 0.3 kcal/mol, while those for **2b** and **2c**, estimated from coalescence temperatures, are about 16.4 and 14.6 kcal/mol, respectively.

Introduction

Monodentate coordination of the $[CHPR_3]^-$ anion is stabilized by the Cp_3U^+ [1-3] and $Cp_2M(X)^+$ fragments (M = Ti, Zr, Hf; X = Cl, C_6H_5, C_2H_5)[4-9] and results in metal–carbon multiple bonds. Since we have developed considerable chemistry about the U–C multiple bond in $Cp_3U{=}CHPR_3$,[10-20] we were interested in studying the requirements and conditions that might lead to other actinide–carbon multiple bonding systems. Structural and chemical similarities between the group IV $Cp_2M(X)$ (Cp = C_5H_5) systems (M = Ti, Zr, Hf; X = Cl) and $Cp^*_2An(X)$ ($Cp^* = C_5Me_5$; An = U, Th; X = Cl)[21] systems suggested that a monodentate ylide coordination might be stabilized by the $Cp^*_2An(X)$ system.

Two types of $Cp_2M(X)$ (M = Ti, Zr, Hf) ylide complexes have been reported. One contains the monodentate $[CHPR_3]^-$ ligand and includes $Cp_2Zr(Cl)[CHP(Me)_3]$,[9] $Cp_2Zr(R)[CHP(Ph)_3]$ (R = C_6H_5,[4] C_2H_5;[7] Me = CH_3, Ph = C_6H_5), $Cp_2M(Cl)[CHP(Ph)_3]$ (M = Zr, Hf),[8] and $Cp_2M(Cl)[CHP(NR_2)_2R']$[5,6] (M = Ti, Zr, Hf; R = C_2H_5 or Me; R′ = $N(C_2H_5)_2$ or Me). In the second type the ylide is chelating: $Cp_2Zr(H)[(CH_2)(CH_2)P(Me)_2]$,[9] $Cp_2Zr(Cl)[(CH_2)(CH_2)P(Me)_2]$,[9] and $Cp_2Zr(Cl)[(CH_2)(CH_2)P(N(C_2H_5)_2)_2]$.[5,22] It has further been observed that some of the second group of complexes convert spontaneously into the first type upon mild heating.[9] We consequently have studied the reaction of $Cp^*_2AnCl_2$ with $Li[(CH_2)(CH_2)PRR']$ to determine if analogous actinide complexes could be prepared. In this paper we report the following reaction

$$Cp^*_2AnCl_2 + Li[(CH_2)(CH_2)PRR'] \rightarrow Cp^*_2An(Cl)[(CH_2)(CH_2)PRR'] + LiCl \quad (1)$$

$$\textbf{1a–c} \text{ or } \textbf{2a–c}$$

1, An = U(IV); **2**, An = Th(IV); **a**, R = Me, R′ =Ph; **b**, R = R′ = Ph; **c**, R = R′ = Me

Only these thermally stable complexes, which contain chelating ylide ligands, are formed.

Experimental Section

Materials and Methods. All procedures were performed under a dry dinitrogen atmosphere by using normal Schlenk techniques, a Vacuum Atmospheres glovebox equipped with an HE-493 Dri-train, or in a high vacuum line. Solvents were dried over sodium benzophenone ketyl and degassed by several freeze–thaw cycles on the high vacuum line. Low-resolution EI mass spectra were recorded on a Varian MAT-311 spectrometer interfaced to an IBM PC. Infrared spectra (4000–600 cm^{-1}) were

---

(1) Cramer, R. E.; Maynard, R. B.; Paw, J. C.; Gilje, J. W. *J. Am. Chem. Soc.* **1981**, *103*, 3589–3590.

(2) Cramer, R. E.; Maynard, R. B.; Paw, J. C.; Gilje, J. W. *Organometallics* **1983**, *2*, 1336–1340.

(3) Cramer, R. E.; Bruck, M. A.; Edelmann, F.; Afzal, D.; Gilje, J. W.; Schmidbaur, H. *Chem. Ber.* **1987**, *121*, 417–420.

(4) Erker, G.; Czisch, P.; Mynott, R.; Tsay, Y. H.; Kruger, C. *Organometallics* **1985**, *4*, 1310–1312.

(5) Schmidbaur, H.; Pichl, R. *Z. Naturforsch.* **1985**, *40B*, 352–356.

(6) Schmidbaur, H.; Pichl, R.; Muller, G. *Angew. Chem., Int. Ed. Engl.* **1986**, *25*, 574–575.

(7) Erker, G.; Czisch, P.; Kruger, C.; Wallis, J. M. *Organometallics* **1985**, *4*, 2059–2060.

(8) Baldwin, J. C.; Keder, N. L.; Strouse, C. E.; Kaska, W. C. *Z. Naturforsch.* **1980**, *35B*, 1289–1297.

(9) Schwartz, J.; Gell, K. I. *Inorg. Chem.* **1980**, *19*, 3207–3211.

(10) Cramer, R. E.; Maynard, R. B.; Paw, J. C.; Gilje, J. W. *Organometallics* **1982**, *1*, 869–871.

(11) Cramer, R. E.; Higa, K. T.; Pruskin, S. L.; Gilje, J. W. *J. Am. Chem. Soc.* **1983**, *105*, 6749–6750.

(12) Cramer, R. E.; Panchanatheswaran, K.; Gilje, J. W. *J. Am. Chem. Soc.* **1984**, *106*, 1853–1854.

(13) Cramer, R. E.; Higa, K. T.; Gilje, J. W. *J. Am. Chem. Soc.* **1984**, *106*, 7245–7247.

(14) Cramer, R. E.; Higa, K. T.; Gilje, J. W. *Organometallics* **1985**, *4*, 1140–1141.

(15) Cramer, R. E.; Panchanatheswaran, K.; Gilje, J. W. *Angew. Chem., Int. Ed. Engl.* **1984**, *23*, 912–913.

(16) Cramer, R. E.; Englehardt, U.; Higa, K. T.; Gilje, J. W. *Organometallics* **1987**, *6*, 41–45.

(17) Cramer, R. E.; Jeong, J. H.; Gilje, J. W. *Organometallics* **1987**, *6*, 2010–2012.

(18) Gilje, J. W.; Cramer, R. E. *Inorg. Chim. Acta* **1987**, *139*, 177–181.

(19) Gilje, J. W.; Cramer, R. E.; Bruck, M. A.; Higa, K. T.; Panchanatheswaran, K. *Inorg. Chim. Acta* **1985**, *110*, 139–143.

(20) Cramer, R. E.; Jeong, J. H.; Gilje, J. W. *Organometallics* **1986**, *5*, 2555–2557.

(21) Cardin, D. J.; Lappert, M. F.; Raston, C. L. *Chemistry of Organo-Zirconium and -Hafnium Compounds*; Ellis Horwood Limited: West Sussex, England, 1986; Chapter 10.

(22) Schmidbaur, H.; Pichl, R.; Muller, G. *Chem. Ber.* **1987**, *120*, 39–44.

0276-7333/89/2308-1192$01.50/0

recorded on a Perkin-Elmer 1430 spectrometer. Diffraction data were collected on Syntex P$\bar{1}$ or a Nicolet R3m/v diffractometers operating at ambient temperature.

Elemental analyses were performed by Schwarzkopf Microanalytical Laboratory, Woodside, NY, or Dornis u. Kolbe Microanalytical Laboratorium, Mülheim, West Germany.

Uranium tetrachloride and thorium tetrachloride were obtained from Pfaltz and Bauer Research Chemicals, and solutions of *n*-butyllithium and methyllithium were obtained from Strem Chemicals. These materials were used as received. Pentamethylcyclopentadiene, Cp*H,[23-25] its Grignard reagent (Mg[Cp*]Cl·THF),[26] the organoactinide reagents Cp*$_2$AnCl$_2$ (An = U or Th),[26] and the lithiated dialkylphosphodimethanide reagents Li[(CH$_2$)(CH$_2$)PRR′] (R and R′ = Me or Ph)[27] were prepared according to literature procedures.

NMR spectra were recorded on a Nicolet NM-300 spectrometer operating in the Fourier transform mode. Chemical shifts were referenced to internal deuterated solvents and then recalculated to TMS = 0.0 ppm. ^{31}P NMR spectra were referenced to external 85% H$_3$PO$_4$. Samples used for the DNMR experiments were about 0.04 M. The subroutines NMCSIM and ITERCAL, which are contained in the Nicolet NMR program package, were used to simulate the low-temperature methylene spectrum of **2a**. DNMR spectra were calculated by using SITE4,[28,29] a locally written program which calculates NMR line shapes in the presence of exchange from the coupled Bloch equations. Line widths of the sharp Cp* signals in the high- and low-temperature spectra of **2** were close to 2 Hz; consequently a natural line width of 2 Hz was assumed in spectral simulations. Thermodynamic activation parameters were calculated with NMREA,[28,29] a locally written program which obtains activation parameters using an unweighted linear least-squares fit on the ln k vs $1/T$ data. Due to temperature-dependent chemical shifts complete line-shape analysis at intermediate exchange rates was not attempted for the methylene region of **2**.

Syntheses. Cp*$_2$U(Cl)[(CH$_2$)(CH$_2$)P(Me)(Ph)] (1a). To 1.0 g (1.7 mmol) of Cp*$_2$UCl$_2$ was added 0.30 g (1.9 mmol, 10% excess) of Li[(CH$_2$)(CH$_2$)P(Me)(Ph)] in about 50 mL of toluene. After stirring for 24 h at room temperature the color had changed from deep red to orange. The orange solution was filtered through a medium-porosity glass frit containing some Celite and reduced in volume to about 5 mL. Approximately 3 mL of hexane was added, and the solution was cooled to −15 °C. After several days orange-red crystals had grown on the sides and bottom of the flask. These were isolated by filtration and washed with 2 × 0.5 mL hexane and dried under high vacuum: yield 0.95 g (80%); mol wt (mass spectrum) *m/e* 695 (calcd), 695 (obsd); ^{1}H NMR (C$_7$D$_8$; 21 °C) δ 0.1 (15 H, s), 0.9 (15 H, s) (Cp*), −14.6 (3 H, d, $J_{\text{P-H}}$ = 12 Hz) (P–Me), 81.5 (1 H, s, br), 78.2 (1 H, s, br) (CH$_2$), −154 (1 H, s, br), −136 (1 H, s, br) (CH$_2$), 9.0 (2 H, t, br) (*o*-Ph), 7.3 (2 H, t, $J_{\text{H-H}}$ = 7 Hz) (*m*-Ph), 6.8 (1 H, t, $J_{\text{H-H}}$ = 7 Hz) (*p*-Ph); IR (thin film on NaCl) 3060 (m), 2975 (m), 2910 (m), 2860 (sh), 1435 (s), 1295 (s), 1260 (s), 1105 (m), 1085 (m), 960 (m), 805 (s), 745 (s) cm^{-1}.

Anal. Calcd for C$_{29}$H$_{42}$UClP: C, 50.11; H, 6.09. Found: C, 49.88; H, 6.18.

Cp*$_2$Th(Cl)[(CH$_2$)(CH$_2$)P(Me)(Ph)] (2a). **2a** was prepared by the general procedure outlined above for **1a** using 2.5 g (4.4 mmol) of Cp*$_2$ThCl$_2$ and 0.75 g (4.7 mmol) of Li[(CH$_2$)(CH$_2$)P(Me)(Ph)]: yield 2.4 g (79%); mol wt (mass spectrum) *m/e* 689 (calcd), 689 (obsd); ^{1}H NMR (C$_7$D$_8$; 21 °C) δ 1.95 (15 H, s), 2.15 (15 H, s) (Cp*), 1.22 (3 H, d, $J_{\text{P-H}}$ = 12 Hz) (P–Me), (0.61–0.23 (4 H, br) (CH$_2$) (exchange broadened, details are listed in Table VII), 7.6 (5 H, m) (Ph); ^{31}P{^{1}H} δ 11.0 (s); IR (thin film on NaCl) 3045 (m), 2975 (m), 2900 (m), 2860 (w, sh), 1435 (st), 1260 (m), 1100 (br), 1085 (sh), 790 (m), 760 (s) cm^{-1}.

Anal. Calcd for C$_{29}$H$_{42}$ThClP: C, 50.55; H, 6.14. Found: C, 50.37; H, 6.11.

Cp*$_2$U(Cl)[(CH$_2$)(CH$_2$)P(Me)$_2$] (1c). **1c** was prepared by the general procedure outlined above for **1a** using 2.7 g (4.7 mmol) of Cp*$_2$UCl$_2$ and 0.48 g (5.0 mmol) of Li[(CH$_2$)(CH$_2$)P(Me)$_2$]: yield 1.7 g (54%); mol wt (mass spectrum) *m/e* 633 (calcd), 633 (obsd); ^{1}H NMR (C$_7$D$_8$; 21 °C) δ 0.2 (30 H, s) (Cp*), −16.2 (6 H, d, $J_{\text{P-H}}$ = 12 Hz) (P–Me), −146 (2 H, s, br) (CH$_2$), 84 (2 H, s, br) (CH$_2$); IR (thin film on NaCl): 2970 (m), 2900 (m), 2850 (sh), 1430 (m), 1295 (m), 1260 (s), 950 (m), 805 (s) cm^{-1}.

Anal. Calcd for C$_{24}$H$_{40}$UClP: C, 45.53; H, 6.37. Found: C, 45.11; H, 5.99.

Cp*$_2$Th(Cl)[(CH$_2$)(CH$_2$)P(Me)$_2$] (2c). **2c** was prepared by the general procedure outlined above for **1a** using 2.7 g (4.7 mmol) of Cp*$_2$ThCl$_2$ and 0.48 g (5.0 mmol) of Li[(CH$_2$)(CH$_2$)P(Me)$_2$]: yield 1.8 g (61%); mol wt (mass spectrum) *m/e* 627 (calcd), 627 (obsd); ^{1}H NMR (C$_7$D$_8$; 21 °C) δ 2.06 (30 H, s) (Cp*), 0.93 (6 H, d, $J_{\text{P-H}}$ = 12 Hz) (P–Me), −0.13 to −0.23 (4 H, br) (CH$_2$) (exchange broadened, details are listed in Table VII); ^{31}P{^{1}H} (C$_7$D$_8$; 21 °C) δ 6.0 (s); IR (thin film on NaCl) 2975 (sh), 2900 (s), 2860 (m), 1430 (m), 1300 (m), 1260 (m), 990 (s), 800 (m) cm^{-1}.

Anal. Calcd for C$_{24}$H$_{40}$ThClP: C, 45.98; H, 6.43. Found: C, 45.22; H, 6.17.

Cp*$_2$U(Cl)[(CH$_2$)(CH$_2$)P(Ph)$_2$] (1b). **1b** was prepared by the general procedure outlined above for **1a** using 4.7 g (8.2 mmol) of Cp*$_2$UCl$_2$ and 2.0 g (9.1 mmol) of Li[(CH$_2$)(CH$_2$)P(Ph)$_2$]: yield 4.8 g (78%); mol wt (mass spectrum) *m/e* 757 (calcd), 757 (obsd:; ^{1}H NMR (C$_7$D$_8$; 21 °C) δ 0.5 (30 H, s) (Cp*), −154 (2 H, s, br) (CH$_2$), 80 (2 H, s, Br) (CH$_2$), 5.5 (6 H, br, *m*-, *p*-Ph), 0.05 (4 H, br, *o*-Ph); IR (thin film on NaCl) 3060 (w), 2975 (m), 2910 (m), 2860 (sh), 1435 (s), 1260 (s), 1100 (m), 1085 (m), 795 (m), 740 (s) cm^{-1}.

Anal. Calcd for C$_{34}$H$_{44}$UClP: C, 53.99; H, 5.88. Found: C, 53.86; H, 5.84.

Cp*$_2$Th(Cl)[(CH$_2$)(CH$_2$)P(Ph)$_2$] (2b). **2b** was prepared by the general procedure outlined above for **1a** using 2.0 g (3.5 mmol) of Cp*$_2$ThCl$_2$ and 0.80 g (3.6 mmol) of Li[(CH$_2$)(CH$_2$)P(Ph)$_2$]: yield 1.9 g (74%); mol wt (mass spectrum) *m/e* 751 (calcd), 751 (obsd); ^{1}H NMR (C$_7$D$_8$; 21 °C) δ 2.00 (30 H, s) (Cp*), 0.68 (2 H, d, $J_{\text{P-H}}$ = 8 Hz) (CH$_2$), 0.502 (2 H, d, $J_{\text{P-H}}$ = 13 Hz) (CH$_2$), 7.6 (10 H, m) (*o*-, *m*-, *p*-Ph); ^{31}P{^{1}H} (C$_7$D$_8$): δ 6.0 (s); IR (thin film on NaCl) 3045 (m), 2975 (sh), 2900 (s), 1435 (s), 1260 (m), 1100 (br), 1085 (m), 790 (s), 760 (s) cm^{-1}.

Anal. Calcd for C$_{34}$H$_{44}$ThClP: C, 54.36; H, 5.90. Found: C, 53.05; H, 5.62.

Collection and Reduction of X-ray Data. Crystals of **1a** and **1b** from the preparations described above were selected, mounted, and sealed in thin-walled glass capillaries under dinitrogen.

A Syntex P$\bar{1}$ four-circle computer-controlled diffractometer with graphite-monochromatized Mo Kα radiation (Kα_1, 0.709 30 and Kα_2, 0.713 59 Å) and a scintillation detector with pulse height analyzer was used for the measurement of diffraction intensities of **1a**. Cell constants were determined by least-squares methods from the centered angular coordinates of 15 intense reflections with 2θ values between 10° and 20° in the triclinic system and between 5° and 18° in the monoclinic system. For **1b**, a Nicolet R3m/v four-circle computer-controlled diffractomer with graphite-monochromatized Mo Kα radiation was employed for the measurement of diffraction intensities. Cell constants were determined by least-squares methods from 36 intense reflections with 2θ values between 7° and 28°. Crystal data, data collection, and refinement parameters are listed in Table I.

For **1a**, atomic scattering factors for P^0, Cl^0, C^0, and H^0 were supplied by SHELX-76,[30] that for U^0 was taken from the literature,[31] and those for **1b** were supplied by SHELXTL PLUS which is part of the Nicolet R3m/v system.

Structure Solution and Refinement. A triclinic and a monoclinic form of **1a** have been isolated (Table I). For the triclinic form a structure solution was obtained with a partial data set (2θ = 3–35°) using a rapid scan rate of 8–24 °/min which gave R = 0.0698 and R_g = 0.0882 (Table I). The triclinic structure was

---

[23] Kohl, F. X.; Jutzi, P. *J. Organomet. Chem.* **1983**, *243*, 119–121.

[24] Threlkel, R. S.; Bercaw, J. E. *J. Organomet. Chem.* **1977**, *136*, 1–5.

[25] Feitler, D.; Whitesides, G. M. *Inorg. Chem.* **1976**, *15*, 466–469.

[26] Fagan, P. J.; Manriquez, J. M.; Maatta, E. A.; Seyam, A. M.; Marks, T. J. *J. Am. Chem. Soc.* **1981**, *103*, 6650–6667.

[27] Manzer, L. E. *Inorg. Chem.* **1976**, *15*, 2567–2568.

[28] SITE4 and NMREA, written by Professor T. T. Bopp, University of Hawaii, were run on a Digital Equipment Corp. PDP 11/45 computer.

[29] For example see: Sandstrom, J. *Dynamic NMR Spectroscopy*; Academic Press: London, 1982; Chapters 2 and 7 and references therein.

[30] SHELX-76, a system of computer programs for X-ray structure determination by G. M. Sheldrick, 1976.

[31] *International Tables for X-Ray Crystallography*; Kynoch Press: Birmingham, England, 1974; Vol. IV, pp 78–87.

Table I. Crystal Data, Data Collection, and Reduction Parameters for $Cp^*_2U(Cl)[(CH_2)(CH_2)P(Ph)R]$ (R = Me, 1a; R = Ph, 1b)

	1a		
	monoclinic	triclinic	1b
formula	$C_{29}H_{42}PClU$	$C_{29}H_{42}PClU$	$C_{34}H_{44}PClU$
fw	695.11	695.11	757.18
space group	$P2_1/c$	$P\bar{1}$	$P2_1/n$
a, Å	13.963 (8)	11.725 (9)	8.763 (8)
b, Å	11.904 (2)	14.625 (7)	19.579 (5)
c, Å	17.541 (3)	8.547 (3)	18.574 (5)
α, deg	90.0	98.41 (4)	90.0
β, deg	103.17 (3)	95.54 (5)	93.604 (4)
γ, deg	90.0	94.78 (5)	90.0
V, Å^3	2839 (2)	1436 (1)	3180 (3)
Z	4	2	4
d, g/cm^3	1.627	1.607	1.585
μ, cm^{-1}	56.08	55.44	49.59
cryst dimens, mm	0.7 × 0.5 × 0.1	0.9 × 0.4 × 0.4	0.9 × 0.5 × 0.3
cryst shape	rectangular prism	irregular	rectangular prism
radiatn (Mo Kα), λ, Å	0.71073	0.71073	0.71073
scan type	$2\theta-\theta$	$2\theta-\theta$	$2\theta-\theta$
scan rate, deg min	4–24	8–24	10–30
2θ range, deg	3–50	3–35	3–35
total observns	4953	2205	2116
unique observns	4609	1916	2019
unique data with $I > 3\sigma(I)$	3526	1552	1751
abs cor factor range	1.01–0.89	none	none
no. of parameters	213	144	132
over determinatn ratio	16.6	10.8	13.3
R^a	0.0402	0.0698	0.0704
$R_g{}^b$	0.0439	0.0882	0.0822

^{a}R = $\sum(|F_c - F_c|)/\sum(F_0)$. $^b R_g = [\sum(|F_o - F_c|)^2/\sum(F_o{}^2)]^{1/2}$.

solved in the space group $P\bar{1}$. The centrosymmetric setting was confirmed by successful least-squares refinement. The final difference Fourier maps of both the triclinic and monoclinic structures showed no peaks greater than 0.5 e/Å^3 except for five peaks between 0.5 and 1.9 e/Å^3 located approximately 1 Å from the uranium atom. Location of hydrogen atoms for the triclinic form was not attempted, nor were they included at their calculated positions. Final positional parameters, temperature factors, and observed and calculated structure factors for the triclinic case are listed in Tables X–XII; bond distances and angles are listed in Table XV (supplementary material).

Several months later we obtained a more complete data set on the same triclinic crystal (2θ = 3–60°) by using a scan rate of 4–24°. Refining the structure using this data set gave R = 0.1198 and R_g = 0.1824. Inspection of the data set showed that the intensity of some reflections differed by large amounts between the two data sets. Apparently, a significant amount of decomposition had occurred between rapid and slow data acquisitions. This was most likely due to oxygen contamination from an incomplete capillary seal. The slow decomposition led to spurious pairs of unrefinable peaks throughout the difference maps. A careful synthesis and subsequent, reproducible crystallization yielded the monoclinic form of **1a**. Metrical parameters reported here are those from the more accurate structure obtained on the monoclinic form.

The structure of the monoclinic crystal was solved in the space group $P2_1/c$ which was indicated by systematic absences. The position of the uranium atom was determined by Patterson methods and the remaining atoms were located from a series of difference Fourier maps and least-squares refinements using SHELX-76.[30] All non-hydrogen atoms were refined anisotropically except for the ring carbons of the pentamethylcyclopentadienide and phenyl groups which were refined isotropically as rigid bodies (C–C(Cp*) = 1.420 Å, C–C(Ph) = 1.395 Å). After an empirical absorption correction using three psi scans with 2θ = 17.69°, 27.91°, and 39.58°, R = 0.0442 and R_g = 0.0499 were obtained.

At this point three weak peaks in the Fourier difference map appeared about 1 Å from the chelate methylene carbons. These were added as hydrogen atoms. A fourth peak appeared in subsequent cycles, and all four peak positions and thermal parameters successfully refined as hydrogen atoms. Other hydrogen atoms were apparent from the difference maps but were placed at calculated positions for CH_3 and C_6H_5 groups with the parameters supplied in SHELX-76.[30] In the final refinement, positions and anisotropic thermal parameters of all non-hydrogen atoms were refined along with the positions of the hydrogen atoms to yield R = 0.0402 and R_g = 0.0439 (Table I). The final cycle of least-squares refinement yielded parameter shifts no greater than 3% of their estimated standard deviation except for seven of the Cp* ring methyl parameters whose shifts ranged from 9 to 79%. Bond lengths and bond angles are shown in Table II. Final positional parameters and temperature factors are listed in Tables III and IV. Observed and calculated structure factors are in Table XIII (supplementary material).

The structure of **1b** was solved in the monoclinic space group $P2_1/n$ which was indicated by systematic absences. The positions of the uranium and phosphorus atoms were determined by

Table II. Bond Lengths (Å) and Selected Bond Angles (deg) for $Cp^*_2U(Cl)[(CH_2)(CH_2)P(Ph)R]$ (R = Me, 1a; R = Ph, 1b)

	bond length^a			bond angle^b	
	1a	1b		1a	1b
U–Cl	2.658 (2)	2.680 (8)	C(1)–U–Cl	138.1 (1)	136.7 (6)
U–C(1)	2.62 (1)	2.62 (3)	C(2)–U–Cl	74.5 (1)	72.8 (6)
U–C(2)	2.58 (1)	2.54 (3)	C(2)–U–C(1)	64.2 (3)	64.6 (8)
P–C(1)	1.74 (1)	1.74 (3)	C(2)–P–C(1)	104.7 (6)	104 (1)
P–C(2)	1.74 (1)	1.77 (3)	C(3)–P–C(1)	110.6 (6)	
P–C(3)	1.77 (1)		C(31)–P–C(1)		109 (1)
P–C(41)		1.82 (2)	C(3)–P–C(2)	108.6 (6)	
P–C(31)	1.809 (6)	1.82 (2)	C(31)–P–C(2)		110 (1)
U–C(11)	2.773 (6)	2.83 (2)	C(31)–P–C(1)	115.1 (3)	
U–C(12)	2.784 (6)	2.80 (2)	C(41)–P–C(1)		112 (1)
U–C(13)	2.792 (6)	2.77 (2)	C(31)–P–C(2)	115.2 (5)	
U–C(14)	2.786 (6)	2.77 (2)	C(41)–P–C(2)		116 (1)
U–C(15)	2.775 (6)	2.81 (2)	C(31)–P–C(3)	102.6 (5)	
U–C(21)	2.781 (8)	2.81 (2)	C(31)–P–C(41)		105 (1)
U–C(22)	2.740 (8)	2.75 (2)	P–C(1)–U	93.3 (3)	94 (1)
U–C(23)	2.741 (8)	2.76 (2)	P–C(2)–U	94.8 (5)	96 (1)
U–C(24)	2.783 (8)	2.83 (2)	Cp_1–U–Cl	97.8	101.2
U–C(25)	2.807 (8)	2.86 (2)	Cp_1–U–C(1)	98.6	103.1
Cp_1–U^a	2.50	2.56	Cp_1–U–C(2)	123.1	125.5
Cp_2–U	2.49	2.63	Cp_2–U–C(1)	98.6	103.1
			Cp_2–U–C(2)	104.0	114.4
			Cp_2–U–Cl	99.6	103.1
			U–C(1)–C(2)–P^b	18.0	11.4
			Cp_1–U–Cp_2	132.6	136.7

^{a} Cp_1 and Cp_2 represent the centroid of the C_5 rings. ^{b} The dihedral fold angle within the four-membered chelate ring.

Table III. Positional and Thermal Parameters of Anisotropically Refined Atoms for $Cp^*_2U(Cl)[(CH_2)(CH_2)P(Ph)(Me)]$ (1a)

atom	x	y	z	U_{11}	U_{22}	U_{33}	U_{23}	U_{13}	U_{12}
U	0.24190 (3)	0.20321 (3)	0.06917 (2)	0.0370 (2)	0.0383 (2)	0.0320 (2)	−0.0020 (2)	0.0040 (1)	0.0028 (2)
Cl	0.1565 (2)	0.1576 (3)	−0.0793 (1)	0.074 (2)	0.073 (2)	0.036 (1)	−0.006 (1)	−0.001 (1)	−0.001 (2)
P	0.1571 (2)	0.0182 (2)	0.1714 (2)	0.049 (2)	0.043 (1)	0.045 (1)	0.003 (1)	0.005 (1)	−0.001 (1)
C(1)	0.2414 (8)	0.1241 (9)	0.2084 (6)	0.050 (6)	0.045 (6)	0.041 (5)	0.001 (5)	0.014 (5)	0.004 (5)
C(2)	0.1556 (9)	0.012 (1)	0.0718 (6)	0.063 (8)	0.056 (7)	0.046 (6)	−0.003 (5)	−0.001 (5)	−0.022 (6)
C(3)	0.0376 (8)	0.055 (1)	0.1815 (8)	0.052 (7)	0.058 (7)	0.083 (8)	0.004 (6)	0.015 (6)	−0.002 (6)

Table IV. Positional and Thermal Parameters for Isotropically Refined Non-Hydrogen Atoms for $Cp^*_2U(Cl)(CH_2)(CH_2)P(Ph)(Me)$ (1a)

atom	x	y	z	U, Å^2
C(11)	0.1336 (5)	0.3539 (6)	1.1359 (3)	0.046 (2)
C(12)	0.0795 (5)	0.3437 (6)	1.0571 (3)	0.046 (2)
C(13)	0.1353 (5)	0.3947 (6)	1.0083 (3)	0.054 (2)
C(14)	0.2239 (5)	0.4364 (6)	1.0571 (3)	0.060 (3)
C(15)	0.2229 (5)	0.4113 (6)	1.1359 (3)	0.046 (2)
C(11M)	0.0903 (8)	0.3419 (9)	1.2063 (6)	0.058 (3)
C(12M)	−0.0220 (8)	0.298 (1)	1.0297 (6)	0.063 (3)
C(13M)	0.0961 (9)	0.418 (1)	0.9226 (7)	0.071 (3)
C(14M)	0.291 (1)	0.516 (1)	1.0298 (8)	0.087 (4)
C(15M)	0.301 (1)	0.439 (1)	1.2089 (8)	0.076 (4)
C(21)	0.4401 (6)	0.2490 (5)	1.0802 (4)	0.063 (3)
C(22)	0.4041 (6)	0.1966 (5)	1.0064 (4)	0.055 (3)
C(23)	0.3835 (6)	0.0823 (5)	1.0199 (4)	0.055 (3)
C(24)	0.4068 (6)	0.0640 (5)	1.1021 (4)	0.054 (3)
C(25)	0.4417 (6)	0.1671 (5)	1.1393 (4)	0.055 (3)
C(21M)	0.494 (1)	0.358 (1)	1.0953 (8)	0.085 (4)
C(22M)	0.399 (1)	0.253 (1)	0.9291 (7)	0.081 (4)
C(23M)	0.358 (1)	−0.008 (1)	0.9592 (8)	0.077 (4)
C(24M)	0.410 (1)	−0.049 (1)	1.1410 (8)	0.078 (4)
C(25M)	0.489 (1)	0.182 (1)	1.2250 (7)	0.075 (4)
C(31)	0.1785 (5)	−0.1147 (5)	1.2228 (4)	0.047 (2)
C(32)	0.2250 (5)	−0.1205 (5)	1.3021 (4)	0.056 (3)
C(33)	0.2332 (5)	−0.2236 (5)	1.3411 (4)	0.061 (3)
C(34)	0.1949 (5)	−0.3209 (5)	1.3007 (4)	0.068 (3)
C(35)	0.1484 (5)	−0.3150 (5)	1.2214 (4)	0.081 (4)
C(36)	0.1403 (5)	−0.2119 (5)	1.1824 (4)	0.079 (4)

Patterson methods, and the remaining atoms were located from a series of difference Fourier maps and least-squares refinements using SHELXTL PLUS. All non-hydrogen atoms were refined anisotropically except all of the carbon atoms of the Cp* and phenyl groups, which were refined isotropically as rigid bodies as described above for **1a**, to yield $R = 0.0704$ and $R_g = 0.0822$ (Table I). A final difference map showed no peaks greater than 0.5 e/Å^3 except for five peaks between 1.5 and 1.9 e/Å^3 located approximately 1.4 Å from the uranium atom. The final cycles of least-squares refinement yielded parameter shifts no greater than 3% of their estimated standard deviations. Bond lengths and bond angles are shown in Table II. Final positional parameters and temperature factors are listed in Tables V and VI. Observed and calculated structure factors are in Table XIV (supplementary material).

Results

Description of the Structure. Perspective drawings of $Cp^*_2(Cl)U[(CH_2)(CH_2)P(Me)(Ph)]$ (**1a**) and $Cp^*_2(Cl)U[(CH_2)(CH_2)P(Ph)_2]$ (**1b**) are shown in Figures 1 and 2, respectively. The bidentate ylide is coordinated to the metal through two U–C σ bonds. The molecule is of the Cp_2ML_3 "bent metallocene" type with a normal ring centroid–U–ring centroid angle of 133° and an average U–C(Cp*) distance, 2.770 (7) Å, within the range found for other actinide–C(Cp*) complexes.[32-36] The Cp* rings are staggered. The average U–C(ylide) distance of 2.60 (1) Å is similar to those we have found in other compounds containing uranium bound to chelating phosphoylide ligands,[37-40] but is longer than uranium–carbon σ bonds found, for example, in $Cp^*_2U(Me)_2$, 2.43 (1) Å.[41] Within the ylide ligand the P–C bond lengths are normal when compared to other chelating phosphoylides.[5,6,37-39,42]

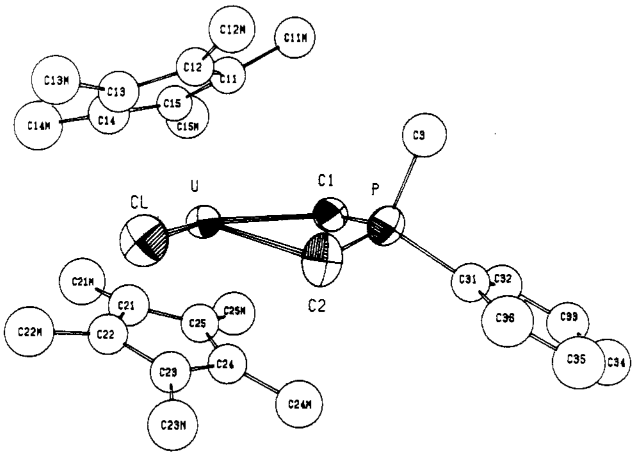

Figure 1. Perspective drawing of $Cp^*_2U(Cl)[(CH_2)(CH_2)P(Me)(Ph)]$ (**1a**).

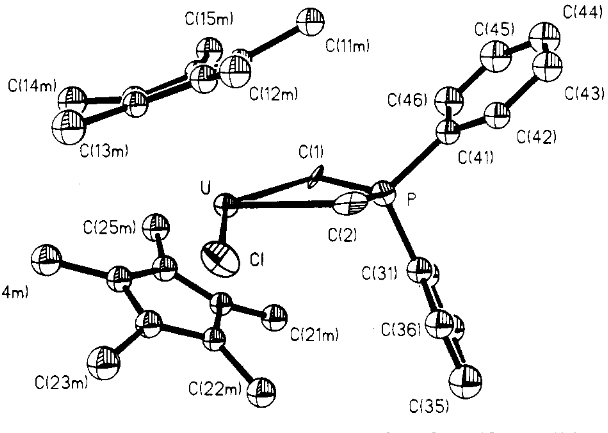

Figure 2. Perspective drawing of $Cp^*_2U(Cl)[(CH_2)(CH_2)P(Ph)_2]$ (**1b**).

The U–Cl distances found in **1a** and **1b**, 2.658 (2) and 2.680 (8) Å, respectively, are slightly longer than those

---

[32] Eigenbrot, C. W.; Raymond, K. N. *Inorg. Chem.* **1982**, *21*, 2653–2660.

[33] Lin, Z.; LeMarechal, J.-F.; Sabat, M.; Marks, T. J. *J. Am. Chem. Soc.* **1987**, *109*, 4127–4129.

[34] Smith, G.; Sabat, M.; Marks, T. J. *J. Am. Chem. Soc.* **1987**, *109*, 1854–1856.

[35] Bruno, J. W.; Smith, G. M.; Marks, T. J.; Fair, C. K.; Schultz, A. J.; Williams, J. M. *J. Am. Chem. Soc.* **1986**, *108*, 40–56.

[36] Marks, T. J.; Day, V. W. in *Fundamental and Technological Aspects of Organo-f-Element Chemsitry*; Marks, T. J., Fragalà, I. L., Eds.; Reidel: Dordrecht, 1985; pp 115–157.

[37] Cramer, R. E.; Maynard, R. B.; Gilje, J. W. *Inorg. Chem.* **1980**, *19*, 2564–2569.

[38] Cramer, R. E.; Maynard, R. B.; Gilje, J. W. *J. Am. Chem. Soc.* **1978**, *100*, 5562–5564.

[39] Cramer, R. E.; Maynard, R. B.; Gilje, J. W. *Inorg. Chem.* **1981**, *20*, 2466–2470.

[40] Cramer, R. E.; Mori, A. L.; Maynard, R. B.; Gilje, J. W.; Tatsumi, K.; Nakamura, A. *J. Am. Chem. Soc.* **1984**, *106*, 5920–5926.

[41] $Cp^*_2U(Me)_2$ crystallizes in the space groups *Fmm*2 (where the Cp* rings are eclipsed: Marks, T. J.; Day, V. W., private communication) and $I4_1/a$ (where the Cp* rings are staggered: Roth, S. Ph.D. Dissertation, University of Hawaii, 1988).

[42] Brauer, D. J.; Kruger, C.; Roberts, P. J.; Tsay, Y.-H. *Chem. Ber.* **1974**, *107*, 3706–3715.

Table V. Positional and Thermal Parameters of Anisotropically Refined Atoms for $Cp^*_2U(Cl)[(CH_2)(CH_2)P(Ph)_2]$ (1b)

atom	x	y	z	U_{11}	U_{22}	U_{33}	U_{23}	U_{13}	U_{12}
U	0.6134 (1)	0.31639 (6)	0.71631 (6)	0.0253 (8)	0.0574 (9)	0.0507 (9)	−0.0003 (8)	−0.0024 (5)	0.0002 (7)
Cl	0.8970 (9)	0.2722 (5)	0.7532 (5)	0.045 (5)	0.114 (8)	0.100 (8)	−0.019 (6)	−0.015 (5)	0.014 (5)
P	0.4071 (8)	0.1783 (4)	0.7045 (4)	0.037 (5)	0.059 (6)	0.063 (6)	−0.0003 (5)	−0.002 (4)	0.006 (5)
C(1)	0.342 (3)	0.262 (1)	0.693 (1)	0.04 (2)	0.03 (2)	0.06 (2)	0.03 (2)	−0.00 (2)	−0.01 (2)
C(2)	0.609 (3)	0.187 (2)	0.707 (1)	0.04 (2)	0.12 (3)	0.04 (2)	0.01 (2)	0.04 (2)	−0.01 (2)

Table VI. Positional and Thermal Parameters for Isotropically Refined Non-Hydrogen Atoms for $Cp^*_2U(Cl)(CH_2)(CH_2)P(Ph)_2$ (1b)

atom	x	y	z	U, Å^2
C(11)	0.593 (2)	0.3037 (9)	0.564 (1)	0.047 (8)
C(12)	0.750 (2)	0.3138 (9)	0.584 (1)	0.066 (9)
C(13)	0.769 (2)	0.3814 (9)	0.611 (1)	0.055 (9)
C(14)	0.623 (2)	0.4130 (9)	0.608 (1)	0.062 (9)
C(15)	0.514 (2)	0.3650 (9)	0.579 (1)	0.059 (9)
C(11M)	0.529 (4)	0.240 (2)	0.523 (2)	0.07 (1)
C(12M)	0.879 (4)	0.260 (2)	0.575 (2)	0.08 (1)
C(13M)	0.925 (4)	0.416 (2)	0.632 (2)	0.09 (1)
C(14M)	0.592 (4)	0.491 (2)	0.613 (2)	0.09 (1)
C(15M)	0.349 (4)	0.381 (2)	0.554 (2)	0.08 (1)
C(21)	0.452 (2)	0.351 (1)	0.837 (1)	0.055 (9)
C(22)	0.602 (2)	0.333 (1)	0.863 (1)	0.052 (8)
C(23)	0.704 (2)	0.384 (1)	0.842 (1)	0.07 (1)
C(24)	0.617 (2)	0.435 (1)	0.803 (1)	0.064 (9)
C(25)	0.461 (2)	0.415 (1)	0.800 (1)	0.07 (1)
C(21M)	0.304 (4)	0.315 (2)	0.862 (2)	0.08 (1)
C(22M)	0.646 (4)	0.274 (2)	0.911 (2)	0.08 (1)
C(23M)	0.869 (4)	0.398 (2)	0.870 (2)	0.09 (1)
C(24M)	0.672 (4)	0.505 (2)	0.784 (2)	0.09 (1)
C(25M)	0.319 (4)	0.454 (2)	0.763 (2)	0.09 (1)
C(31)	0.348 (3)	0.146 (1)	0.790 (1)	0.065 (9)
C(32)	0.195 (3)	0.155 (1)	0.806 (1)	0.08 (1)
C(33)	0.145 (3)	0.131 (1)	0.871 (1)	0.09 (1)
C(34)	0.247 (3)	0.099 (1)	0.921 (1)	0.10 (1)
C(35)	0.400 (3)	0.090 (1)	0.905 (1)	0.11 (1)
C(36)	0.450 (3)	0.113 (1)	0.840 (1)	0.08 (1)
C(41)	0.323 (3)	0.120 (1)	0.637 (1)	0.058 (9)
C(42)	0.403 (3)	0.063 (1)	0.616 (1)	0.062 (9)
C(43)	0.337 (3)	0.019 (1)	0.564 (1)	0.08 (1)
C(44)	0.191 (3)	0.032 (1)	0.533 (1)	0.10 (1)
C(45)	0.111 (3)	0.090 (1)	0.554 (1)	0.11 (1)
C(46)	0.177 (3)	0.134 (1)	0.606 (1)	0.09 (1)

found in Cp_3UCl, 2.56 (2) Å,[43] and Cp''_2UCl_2 (Cp'' = $C_5H_3(SiMe_3)_2$), 2.579 (2) Å,[44] but are similar to the 2.69 Å U–Cl distance found in $Cp^*_2UCl_2(pz)$ (pz = pyrazole)[45] and the shorter of the two statistically different, 2.658 (5) and 2.730 (4) Å, U–Cl distances found in $Cp^*_2UCl_2(HNPPh_3)$.[46] In addition, short intramolecular nonbonding contacts of 3.20 and 3.36 Å found between Cl and C13M and Cl and C23M are less than the sum of the van der Waals radii for Cl and C atoms (1.80 Å (Cl) + 1.70 Å (C) = 3.50 Å).[47] The long U–Cl distances and the short nonbonding contacts probably reflect steric crowding within the equatorial girdle of $Cp^*_2AnL_3$ complexes.

In other structurally characterized metal–ylide complexes the conformation of four-membered chelating phosphoylide rings vary from planar to configurations which are folded by as much as 44°.[37-39,42] In **1a** the U–C–P–C chelate ring is folded with an 18.0° dihedral angle between the C(1)–U–C(2) and C(1)–P–C(2) planes and the phosphorus is displaced 0.3 Å below the C(1)–U–C(2) plane. The analogous dihedral angle in **1b** is 11.0°. These are similar to the 17.7° and 11.0° fold angles found in the chelate rings of $CpU[(CH_2)(CH_2)P(Ph)_2]_3$.[40] The difference in these fold angles between **1a** and **1b** probably reflects intramolecular steric interactions. In **1a**, steric repulsion between C24M and the *P*-phenyl group forces the *P*-methyl into close contact between C11M and C12M, resulting in the 18.0° dihedral fold angle. In **1b**, the second phenyl group on phosphorus cannot "fit" between the two Cp* methyls; hence a smaller chelate fold angle is encountered in **1b**. Close intramolecular nonbonding contacts are listed in Table IX (supplementary material).

Table VII. ^1H NMR Spectral Data for the $P–CH_2$ Region of $Cp^*_2An(Cl)[(CH_2)(CH_2)PRR']$ Complexes[a,b]

R, R′	An	δ	P–CH₂	
Me, Ph	Th (**2a**)[c]	0.54	(1 H_a, ddd)	$^2J_{P-Ha}$ = 9.0 Hz $^2J_{H_aH_b}$ = −13.7 Hz
		0.05	(1 H_b, dd)	$^2J_{P-H_b}$ = 7.6 Hz
		0.03	(1 H_c, ddd)	$^2J_{P-H_c}$ = 13.8 Hz $^2J_{H_cH_d}$ = −13.7 Hz $^4J_{H_aH_c}$ = 3.7 Hz
		0.22	(1 H_d, dd)	$^2J_{P-H_d}$ = 13.6 Hz
	U (**1a**)	82	(1 H_a, br)	
		78	(1 H_b, br)	
		−136	(1 H_c, br)	
		−154	(1 H_d, br)	
Ph, Ph	Th (**2b**)[d]	0.68	(2 H, d)	$^2J_{P-H}$ = 7.8 Hz
		0.50	(2 H, d)	$^2J_{P-H}$ = 13.2 Hz
	U (**1b**)	80	(2 H, br)	
		−154	(2 H, br)	
Me, Me	Th (**2c**)[c]	0.06	(2 H, d)	$^2J_{P-H}$ = 8.0 Hz
		−0.10	(2 H, d)	$^2J_{P-H}$ = 13.4 Hz
	U (**1c**)	84	(2 H, br)	
		−146	(2 H, br)	

[a] Recorded in toluene-d^8 (300 MHz). Chemical shifts are recorded in ppm from Me_4Si. [b] Abbreviations: d, doublet; br, broad. [c] Recorded at −45 °C; see Figure 4. [d] Recorded at −1 °C. [e] Recorded at −15 °C.

In **1a** and **1b** the three equatorial donor atoms C(1), C(2), and Cl and the uranium atom are not coplanar. The dihedral angle between the Cl–U–C(1) plane and the Cl–U–C(2) plane in **1a** and **1b** are 11° and 8°, respectively, with the chlorides displaced about 0.3 Å from the C(1)–U–C(2) plane. The angles in the equatorial girdle Cl–U–C(2), Cl–U–C(1), and C(2)–U–C(1) are, within 2σ, the same in **1a** and **1b** (Table II). These are nearly identical with the C–U–C angles of $[(\mu\text{-}CH)(CH_2)P(Ph)_2U(C_5H_5)_2]_2$[37,38] and to the corresponding angles in the similar group IV complex $[Cp_2Zr(Cl)(CH_2)(CH_2)P(N(C_2H_5)_2)_2]$.[22]

NMR. The NMR spectra of **1** and **2** can be interpreted in terms of the solid-state structures of **1a** and **1b**. **1a–c** are paramagnetic uranium(IV) complexes ($5f^2$ electron configuration) which exhibit a wide range of chemical shifts (Table VII). For **1b** the Cp* resonance is observed at 0.05 ppm and the two CH_2 groups, which are nonequivalent, give rise to two separate resonances, one at 80 ppm and the other at −154 ppm. While it is impossible to unambiguously assign the resonances of specific methylene groups, a somewhat similar stereochemistry is encountered in $[(\mu\text{-}CH)(CH_2)P(Ph)_2U(C_5H_5)_2]_2$[37,38] where the CH_2 group occupies an outer position in a Cp_2UXY_2 type complex and resonates at 88 ppm. The hydrogen on the inner μ-CH resonates at −108 ppm.[39] By analogy the 80 ppm resonance in **1b** can be assigned tenatively to the outer CH_2 and the −154 ppm resonance to the CH_2 group in the middle

---

(43) Wong, C.; Yen, T.; Lee, T. *Acta. Crystallogr.* **1965**, *18*, 340.
(44) Lappert, M. F.; Atwood, J. L., private communication.
(45) Eigenbrott, C. W.; Raymond, K. N. *Inorg. Chem.* **1982**, *21*, 2653–2660.
(46) Gilje, J. W.; Roth, S.; Cramer, R. E., manuscript in preparation.
(47) Bondi, A. *J. Phys. Chem.* **1964**, *68*, 441.

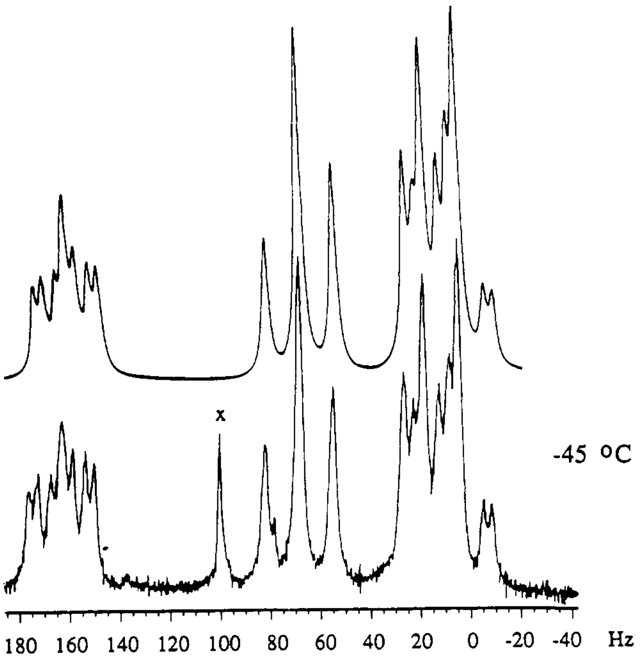

Figure 3. Low-temperature ^1H NMR (300 MHz; C_7D_8, -45 °C) of the P–CH_2 region of $Cp^*_2Th(Cl)[(CH_2)(CH_2)P(Me)(Ph)]$ (**2a**): top, calculated; bottom, experimental (x = impurity).

position. Similar assignments, summarized in Table VII, have been made for **1c**. With **1a** a more complicated spectrum is encountered. Because the phosphorus atom is unsymmetrically substituted, the two Cp* groups in **1a** are nonequivalent and give rise to separate resonances at 0.1 and 0.9 ppm. Similarly separate resonances at 82, 78, −136, and −154 ppm are observed for the four diastereotopic protons within the two CH_2 groups.

The diamagnetic thorium complexes are all fluxional and are in the intermediate exchange region at room temperature. Spectra obtained at low temperature, however, are consistent with the static structures of **1a** and **1b**. The low-temperature spectrum of the CH_2 region of **2a** is complex. All four methylene protons are nonequivalent and give rise to a second order ABCDX spectrum (Figure 3). Low power homonuclear decoupling (spin tickling) at −5 °C and spectral simulation in the slow–intermediate exchange region was employed over the 240 Hz methylene region of **2a** to confirm the assignment, chemical shifts, and H–H coupling and P–C–H coupling constants of each ABX quartet and confirmed that the peak at 0.33 ppm (Figure 3) is due to an impurity. The geminal coupling constants for the downfield H_a–H_b and for the upfield H_c–H_d pair are −13.7 Hz and are accompanied by small and large P–C–H coupling constants, respectively. An additional 3.7 Hz coupling, observed in one downfield set and in one upfield set, is attributed to four-bond H_a–H_c "ω" coupling between the equatorial protons of the four-membered chelate ring (Scheme I).[48] Spectral parameters are listed in Table VII.

As with **1**, the assignment of the methylene groups to the middle or outer position in the equatorial girdle is ambiguous. However, by analogy to the very similar spectrum of $Cp_2Zr(H)[(CH_2)(CH_2)PMe_2]$, where the downfield resonance is assigned to the outer methylene group on the basis of coupling with the hydride ligand,[9] the downfield CH_2 signals in the spectra of **2** probably arise from the outer methylene proton resonances. The two quite different P–C–H coupling constants for the two methylene groups in **2** are analogous to trends in similar group IV transition-metal complexes.[5,9,22] In particular, the smaller P–C–H coupling of 6–7 Hz is always found for the CH_2 group which resonates downfield and the larger P–C–H coupling of 11–14 Hz for the one which resonates at higher field. As previously discussed,[9] the origin of these differences is not certain and may arise from either electronic or steric effects.

Scheme I. Exchange Mechanism for the Fluxional Behavior of 1 and 2

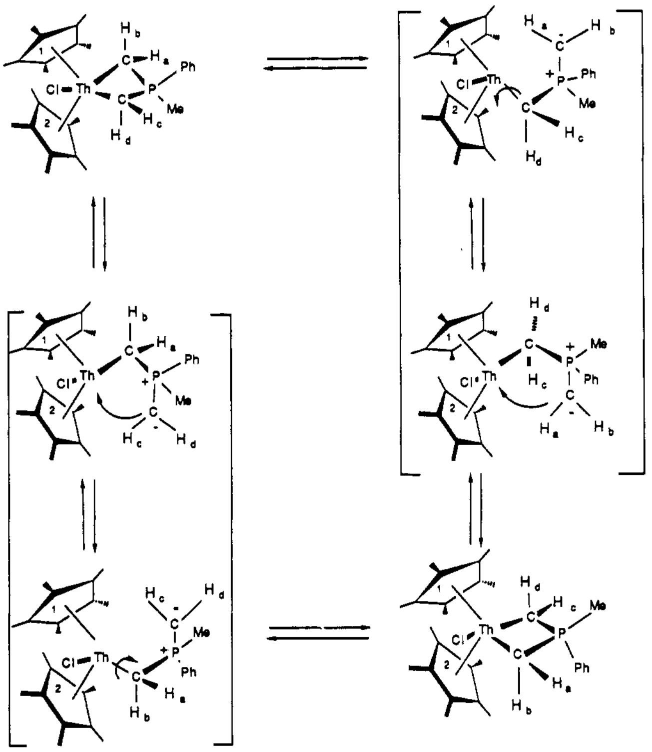

Temperature-dependent chemical shifts found in the methylene region of **2** preclude complete line-shape analysis. For **2a**, only one proton of each P–CH_2 (those mutually coupled by 3.7 Hz) shows a significant variation in chemical shift between −60 and −16 °C. The chemical shifts of the other two P–CH_2 protons do not change significantly over this temperature range. As the temperature is raised, the largest shift is 0.7 Hz/°C (in the upfield direction) for the downfield signal of **2a** at 0.54 ppm (Figure 4), while a 0.3 Hz/°C shift (in the downfield direction) is observed for the proton on the opposite methylene group which resonates at 0.03 ppm. These shifts are accompanied by very sharp peaks, and the line shapes cannot be duplicated by calculated DNMR spectra without changing the slow-exchange chemical shifts of H_a and H_c. This effect is also observed in **2b** and **2c** but only in the upfield set of P–CH_2 resonances. The magnitudes of the shifts found in **2a** seem to be correlated with those of about 0.6 Hz/°C for the dimethyl compound **2c** and 0.3 Hz/°C for the diphenyl compound **2b**. The source of this temperature dependency could be due to solvation, conformational equilibria, or agostic interactions of the CH_2 protons with the thorium center. However, we are unable to offer a convincing explanation.

The magnetically nonequivalent Cp* groups of $Cp^*_2Th(Cl)[(CH_2)(CH_2)P(Me)(Ph)]$ (**2a**) give rise to two peaks (1.97 and 2.15 ppm) at low temperature which broaden, coalesce (T_c = 40 °C), and sharpen to a single peak at 2.00 ppm as the temperature is raised. The four

---

[48] N. S. Bhacca, D. H. Williams *Applications of NMR Spectroscopy in Organic Chemistry*; Holden-Day Publishing Co., Inc: San Francisco, 1964; Chapter 5.

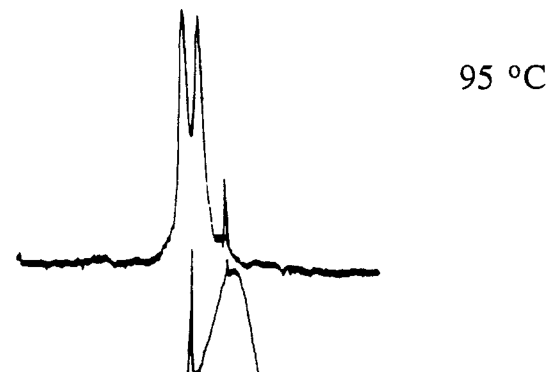

Figure 4. Variable-temperature ^1H NMR (300 MHz; C_7D_8) of the P–CH_2 region of $Cp^*_2Th(Cl)[(CH_2)(CH_2)P(Me)(Ph)]$ (**2a**) (x = impurity).

nonequivalent P–CH_2 protons that are observed in the low-temperature spectrum of **2a** undergo a more complex temperature dependency but at 95 °C are in fast exchange and give rise to a sharp A_4X doublet (Figure 4). The low-temperature spectra of **2b** and **2c** show the expected A_2B_2X splitting in the CH_2 region. As the temperature is raised, these signals broaden, coalesce (T_c = 60 °C (**2b**), 21 °C (**2c**)), and finally re-emerge as an A_4X doublet [$\delta_{av} = (\delta_A + \delta_B)/2 = -0.02$ ppm (**2b**), 0.09 ppm (**2c**); $J_{av} = (J_{AX} + J_{BX})/2 = 10.7$ Hz (**2b**), 10.5 Hz (**2c**)]. In the case of **2a** and **2c**, the P(Me) doublet does not change over the temperature range.

Discussion: Solution Dynamics. Since the DNMR data are not sensitive to concentration changes and since a dissociative ionic process is unlikely in the aromatic hydrocarbon solvents used for the NMR experiments, an intramolecular exchange is probably responsible for the temperature dependency of the NMR spectra of 2. Several pathways can be envisioned for the exchange of the inner and outer CH_2 groups in these molecules. Reversible α-proton transfer which would have precedent in the α-hydrogen transfer which may occur during the formation of Cp_3UCHPR_3,[1-3] $Cp_2Zr(Cl)(CHP(Me)_3)$,[9] and $Cp_2Zr(Cl)[CHP(Me)(N(C_2H_5)_2)_2]$[5,22] can be eliminated because it would also interchange the methylene protons with the *P*-methyl protons in **2a** and **2c**. Since the *P*-methyl doublet is temperature invariant, in the spectra of both **2a** and **2c**, α-hydrogen transfer is not rapid on the NMR time scale.

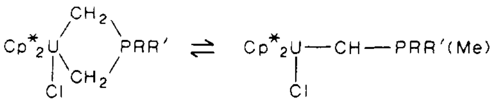

A simple 180° rotation of the chelate without bond dissociation or proton transfer would also interchange the outer and the inner CH_2 positions. However, the geminal protons within each CH_2 group would not be exchanged and the high-temperature ^1H NMR spectrum of **2a** would be an AA′BB′ portion of an AA′BB′X multiplet. In fact, at high temperatures all four phosphorus methylene protons in **2a** appear as the A portion of an A_4X spectrum.

Scheme I describes a third mechanism that can account for the observed fluxional behavior. Dissociation of a methylene group from the metal followed by Th–C and P–C rotation and recombination will equivalence the Cp* groups and the geminal protons on the methylene group which dissociates. The protons on the methylene group which remains coordinated to the metal do not equivalence with each other nor with the second methylene group until that CH_2 group undergoes an analogous dissociation, rotation, and recombination.

Exchange of the Cp* groups in **2a** is a simple two-site exchange. Spectral simulations of the Cp* region of **2a** throughout the temperature range 7–95 °C were calculated as a function of exchange rates with the program SITE4.[28,29] An Arrhenius plot gave $\Delta G^{\ddagger} = 15.4 \pm 0.3$ kcal/mol. Since the Cp* groups in **2b** and **2c** are magnetically equivalent, the rate constant was estimated from the coalescence temperature of the CH_2 resonances using $k = \pi\, \delta\nu/(2^{1/2})$.[29] At T_c, $\Delta G^{\ddagger}$ was calculated for **2b** (T_c = 60 °C) and **2c** (T_c = 21 °C) to be about 16.4 and 14.6 kcal/mol, $\Delta G^{\ddagger}$ for **2a** (T_c = 40 °C) estimated from the coalescence expression, 15.4 kcal/mol, is in good agreement with the value obtained from line-shape analysis.

The ^1H NMR spectrum of $Cp_2Zr(Cl)[(CH_2)(CH_2)P(Me)_2]$ shows a similar temperature dependency ($\Delta G^{\ddagger} \approx 15.5$ kcal/mol).[9] However, it is interesting to note that above the 50 °C coalescence temperature of the P–CH_2 groups, α-hydrogen transfer results in a smooth, irreversable isomerization to $Cp_2Zr(Cl)(CHP(Me)_3)$.[9] This is in contrast to the Cp^*_2An systems 1 and 2 where no rearrangement was detected at 100 °C over several hours.

Discussion

While many organometallic complexes of phosphorus ylides exist with a variety of transition metals,[49-51] with most of the lanthanides,[52-54] and with the actinide uranium,[1-3,37-40] this is the first report of an ylide complex of thorium.

A solution of $Cp^*_2AnCl_2$ (An = U, Th; Cp* = C_5Me_5) treated with 1 equiv of $Li[(CH_2)(CH_2)PRR']$ (R, R′ = Me or Ph) in toluene at ambient temperature for 1 day forms $Cp^*_2An(Cl)[(CH_2)(CH_2)PRR']$ (**1a–c**) and (**2a–c**) in good yield, according to eq 1.

When either $Cp^*_2AnCl_2$ or $Li[(CH_2)(CH_2)PRR']$ is used in excess, only $Cp^*_2An(Cl)[(CH_2)(CH_2)PRR']$ along with unreacted starting materials is isolated. Thus, we have seen no evidence for the replacement of the second chloride

---

(49) Schmidbaur, H. *Acc. Chem. Res.* **1975**, *8*, 62–70.

(50) Kaska, W. C. *Coord. Chem. Rev.* **1983**, *48*, 1–58.

(51) Schmidbaur, H. *Angew. Chem., Int. Ed. Engl.* **1983**, *22*, 907–927.

(52) Schumann, H.; Reier, F. W. *J. Organomet. Chem.* **1981**, *209*, C10–C12.

(53) Schumann, H.; Reier, F. W. *J. Organomet. Chem.* **1982**, *235*, 287–294.

(54) Schumann, H. *Angew. Chem., Int. Ed. Engl.* **1984**, *23*, 474–493.

Organometallics 1989, *8*, 1199–1206

or of a Cp* ligand by an ylide moiety. This behavior should be contrasted to reactions of Cp_3AnCl with $Li[(CH_2)(CH_2)PRR']$ where no evidence of $Cp_2An(ylide)Cl$ has been observed and where products are very dependent upon the metal and reaction stoichiometry. With Cp_3UCl several complexes have been characterized:[1-3,37-40] and with

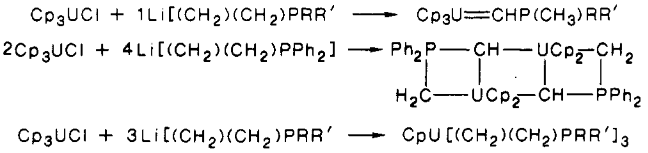

$$Cp_3UCl + 1Li[(CH_2)(CH_2)PRR'] \longrightarrow Cp_3U{=}CHP(CH_3)RR'$$

$$2Cp_3UCl + 4Li[(CH_2)(CH_2)PPh_2] \longrightarrow \begin{array}{cccc} Ph_2P & CH & UCp_2 & CH_2 \\ H_2C & UCp_2 & CH & PPh_2 \end{array}$$

$$Cp_3UCl + 3Li[(CH_2)(CH_2)PRR'] \longrightarrow CpU[(CH_2)(CH_2)PRR']_3$$

the Cp_3ThCl system two chelating ylides can be attached to a Cp_2Th fragment:[55]

$$Cp_3ThCl + 2Li[(CH_2)(CH_2)PPh_2] \rightarrow Cp_2Th[(CH_2)(CH_2)PPh_2]_2$$

Perhaps these differences reflect the greater basicity of Cp*, which makes it less prone to dissociate, and the greater size of this ligand, which prevents the variety of coordination modes encountered with the Cp system.

While there are similarities between the $Cp^*{}_2An$ complexes and Cp_2M complexes of early transition metals,[21,22] **1** and **2** are more thermally stable than their transition-metal counterparts. Both **1** and **2** survive heating to at least 100 °C for several hours while $Cp_2(H)Zr[(CH_2)(CH_2)P(Me)_2]$ rapidly decomposes at 85 °C, $Cp_2(Cl)Zr[(CH_2)(CH_2)P(Me)_2]$ rearranges smoothly to $Cp_2(Cl)Zr{=}CHP(Me)_3$ within 12 h at 50 °C,[9] and $Cp_2(Cl)Zr[(CH_2)(CH_2)P(NEt_2)_2]$, whose structure is analogous to **1**, is in equilibrium with $[Cp_2(Cl)Zr{=}CHP(NEt_2)_2(Me)]$.[6,22] These data indicate that the ylide ligand is more prone to serve as a monodentate $[CHPR_3]^-$ ligand with $Cp_2(X)M$ complexes than with the analogous $Cp^*{}_2(X)An$ complexes.

Acknowledgment. The support of this work by the National Science Foundation, Grant CHE 85-19289 (J. W.G. and R.E.C.), and by the donors of the Petroleum Research Fund, administered by the American Chemical Society, is gratefully acknowledged. The support of the Alexander von Humboldt Foundation through a Feodor Lynen Followship (F.E.) is gratefully acknowledged. We are grateful to Professor T. T. Bopp for the programs SITE4 and NMREA and the many helpful discussions of the NMR data.

Registry No. **1a**, 119743-15-6; **1b**, 119743-16-7; **1c**, 119743-17-8; **2a**, 119743-18-9; **2b**, 119743-19-0; **2c**, 119743-20-3; $Cp^*{}_2UCl_2$, 67506-89-2; $Li[(OH_2)(CH_2)p(Me)(Ph)]$, 59983-61-8; $Cp^*{}_2ThCl_2$, 67506-88-1; $Li[(CH_2)(CH_2)p(Me)_2]$, 21752-68-1; $Li[(CH_2)(CH_2)P(Ph)_2]$, 59983-62-9.

Supplementary Material Available: Tables of positional and thermal parameters for the hydrogen atoms of the monoclonic form of **1a**, intramolecular nonbonded distances for **1a** and **1b**, positional and thermal parameters of anisotropically refined non-hydrogen atoms of the triclinic form of **1a**, positional and thermal parameters of isotropically refined non-hydrogen atoms of the triclinic form of **1a**, and bond lengths and angles for the triclinic form of **1a** (5 pages); listings of observed and calculated structure factors for the triclinic form of **1a**, the monoclinic form of **1a**, and **1b** (40 pages). Ordering information is given on any current masthead page.

---

(55) Gilje, J. W.; Cramer, R. E.; Hitt, J.; Chung, T. D. Y., unpublished results.

Competitive Nucleophilic Aromatic Substitution and Haloarene Reduction in the Synthesis of Bimetallic π-Arene Complexes: The Structural Characterization of $[Et_4N][(\eta^6\text{-}\{(CO)_5W\}C_6H_5)Cr(CO)_3]$

Joseph A. Heppert,* M. Elizabeth Thomas-Miller, Devin M. Scherubel, Fusao Takusagawa, Mark A. Morgenstern, and Mohammad R. Shaker[1]

Department of Chemistry, University of Kansas, Lawrence, Kansas 66045

Received September 6, 1988

Collman's reagent, $[Fe(CO)_4]^{2-}$, reacts with $(\eta^6\text{-}ClC_6H_5)Cr(CO)_3$ to produce $[(\eta^6\text{-}\{(CO)_4Fe\}C_6H_5)Cr(CO)_3]^-$ in THF/*N*-methyl-2-pyrrolidinone solvents, while $[M(CO)_5]^{2-}$ (M = Cr or W) reacts with $(\eta^6\text{-}FC_6H_5)Cr(CO)_3$ in THF at 0 °C to form analogous $[(\eta^6\text{-}\{(CO)_5M\}C_6H_5)Cr(CO)_3]^-$ complexes. The products are isolated as yellow-orange crystalline $[Et_4N]^+$ salts from acetone or methylene chloride and are somewhat air sensitive in both solution and the solid state. Spectroscopic data indicate that the molecules adopt a classical η^6-arene structure, as opposed to the alternate possible η^5-cyclohexadienide carbene valence form. This supposition is confirmed by an X-ray crystallographic study of $[Et_4N][(\eta^6\text{-}\{(CO)_5W\}C_6H_5)Cr(CO)_3]$, which displays a typical $W{-}C_{Ar}$ σ-bond interaction and a minimal distortion of the planarity of the arene. The reaction of $[M(CO)_5]^{2-}$ (M = Cr or W) with $(\eta^6\text{-}ClC_6H_5)Cr(CO)_3$ results in the exhaustive reductive dehalogenation of the chlorobenzene substrate to $(\eta^6\text{-}C_6H_6)Cr(CO)_3$. This later reaction is in keeping with anticipated higher reactivity and reducing power of the $[M(CO)_5]^{2-}$ anions. Crystal data for $[Et_4N][(\eta^6\text{-}\{(CO)_5W\}C_6H_5)Cr(CO)_3]$ at 20 °C: $a = 11.599$ (3) Å, $b = 10.562$ (2) Å, $c = 20.369$ (5) Å, $Z = 4$, $D_{calcd} = 1.782$, space group $Pca2_1$ and $R(F) = 0.0352$, $R_w(F) = 0.0583$ for 1698 reflections.

Introduction

Complexes bearing $(\eta^6\text{-arene})Cr(CO)_3$ subunits have been widely studied because of the unique modes of reactivity that the $Cr(CO)_3$ template engenders in the arene ligand.[2] Although the increased electrophilicity of the aromatic carbon centers is among the most interesting and widely exploited facets of (π-arene)chromium chemistry,

---

[1] Summer participant, University of Kansas Undergraduate Research Program. Current address: Department of Chemistry, Idaho State University, Pocatello, ID.

[2] Watts, W. E. *Comprehensive Organometallic Chemistry*; Wilkinson, J., Ed.; Pergamon Press: London, 1982; Chapter 59.

0276-7333/89/2308-1199$01.50/0